

Dynamic Structural Behavior and Anion-Responsive Tunable Luminescence of a Flexible Cationic Metal–Organic Framework**

Biplab Manna, Abhijeet K. Chaudhari, Biplab Joarder, Avishek Karmakar, and Sujit K. Ghosh*

Dedicated to Professor K. N. Ganesh on the occasion of his 60th birthday

Microporous metal–organic frameworks (MOFs) are of great current interest, because of their fascinating architectures and their wide range of potential applications, especially in gas storage, chemical separation, drug delivery, catalysis, enantioseparation, optical properties, chemosensing etc.^[1] Mostly second-generation rigid porous materials showed exotic results in the aforementioned areas, with their intact, stable, and rigid porosity of the overall framework.^[2] Recently, Kitagawa and co-workers, as well as and other research groups explored the third generation of soft materials and their advantages over rigid porous frameworks.^[3] It is particularly important to study the guest-responsive structural dynamism of such materials. Flexible soft porous materials are sensitive to the chemical environment and undergo structural variations depending upon the nature of guest molecules inside the framework.^[4] Among various MOFs, cationic MOFs have advantages over others in the design of dynamic frameworks. Cationic MOFs are often made of neutral ligands and metal ions, so extra-framework anions usually occupy the framework void or are weakly coordinated to the metal centers.^[5] Exchanging anions inside the framework with other anions of different shape and size may lead to changes in structure and physical properties.^[6] Luminescent MOFs with switchable properties are of great interest because of their potential applications in chemical sensors.^[7] Luminescent cationic MOFs with extra-framework anions offer a dynamic framework and tunable luminescent behavior by exchanging these extra-framework anions with other anions of different shape, size, and coordinating nature. Until now, great progress has been made on separation and other applications of dynamic frameworks, but luminescent response to guest molecules/anions was rarely reported in conjunction with structural dynamism.^[8]

Herein, we report a porous MOF that is made of one-dimensional (1D) coordination polymers of Zn^{II} and a newly designed neutral N-donor organic ligand (L) with extra-framework nitrate anions, and shows interesting guest- and

anion-dependent structural dynamism. Dynamic structural behavior has been demonstrated by single-crystal-to-single-crystal (SCSC) structural transformation. The compound shows slow opening of the framework upon guest inclusion and size-selective sorption of hydrophobic guest molecules. Anions of the framework are easily exchangeable, and the compound shows interesting anion-responsive tunable luminescent behavior.

Linear bichelating ligand **L** is synthesized by Schiff-base condensation of 4,4'-ethylenedianiline and 2-pyridine-carboxaldehyde in high yield (see the Supporting Information). The combination of **L** and Zn(NO₃)₂ in a solvent system of CH₂Cl₂/MeOH and benzene afforded yellow rod-shaped single crystals of compound **1a** [Zn(L)(MeOH)₂-(NO₃)₂·xG]_n (in which G are disordered guest molecules). Single-crystal analysis of the complex showed the formation of a 1D chain structure. These 1D chains are H-bonded with other chains through uncoordinated anions and solvent molecules, leading to an H-bond-based 3D structure with 1D pore channels. A noteworthy feature of compound **1a** is that, when the crystals of **1a** were removed from the mother liquor and kept at room temperature for one hour, they showed a drastic structural transformation of the network without losing their crystalline nature. Single-crystal analysis of those crystals showed large differences in unit-cell parameters, and complete structural analysis showed that two coordinated MeOH solvent molecules per Zn^{II} escaped and were replaced by two H₂O molecules to form a new phase, **1** [Zn(L)(H₂O)₂](NO₃)₂·2H₂O]_n. Although the coordination networks of complexes **1a** and **1** are very similar, the overall structure, shape, and size of the channels are very different (Figure 1).

A single-crystal X-ray diffraction (SC-XRD) study showed that compound **1a** crystallized in the monoclinic

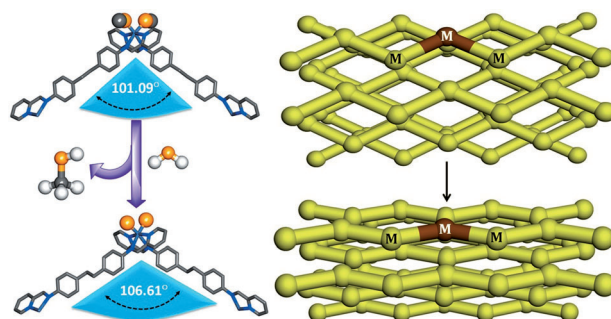


Figure 1. Crystal structures of compound **1a** (top) and **1** (bottom) showing coordination environment (left) and overall framework (right). Free solvents and anions are omitted for clarity.

[*] B. Manna, A. K. Chaudhari, B. Joarder, A. Karmakar, Dr. S. K. Ghosh
Indian Institute of Science Education and Research (IISER)
Homi Bhabha Road, Pashan, Pune-411008 (India)
E-mail: sghosh@iiserpune.ac.in
Homepage: <http://www.iiserpune.ac.in/~sghosh/>

[**] B.M. is thankful to CSIR for a research fellowship. We are grateful to IISER Pune, DAE (project no. 2011/20/37C/06/BRNS) and DST (project no. GAP/DST/CHE-12-0083) for financial support.

Supporting information for this article is available on the WWW under <http://dx.doi.org/10.1002/ange.201206724>.

system, space group $C2/c$. The asymmetric unit of **1a** consists of one-half of each Zn^{II} and **L**, one coordinated methanol, one disordered nitrate anion, and disordered solvents. Each metal ion exhibits a six-coordinated distorted octahedral geometry with an N_4O_2 donor set, bonding from two different **L** with four nitrogen-coordinating sites, and the remaining two coordinating sites are occupied by two methanol molecules. The Zn^{II} –N(pyridine), Zn^{II} –N(aliphatic), and Zn^{II} –O distances are 2.156(3), 2.217(3), and 2.081(3) Å, respectively. At both sides of **L**, a nitrogen atom from the *ortho* position of the aromatic ring and one aliphatic nitrogen atom binds to Zn^{II} in a bidentate fashion. Coordination from both sides of the ligand **L** extended the structure to a 1D chain in zigzag manner (see Figure S1 in the Supporting Information). According to the packing diagram, the cationic chains of compound **1a** form 1D channels along the *c* axis, which encapsulate disordered nitrate ions and solvent molecules. SCSC transformation analysis showed that the crystal system of compound **1** is the same as that of **1a** (monoclinic), but the space group changed to $P2_1/n$. The coordination environment around Zn^{II} remains almost unchanged with a similar N_4O_2 donor set, but coordinated methanol molecules are now replaced by water molecules. Bond lengths and angles around Zn^{II} are also very similar. The 3D packing structure of the cationic chains of **1** show that this compound also formed a channel along the *a* axis, which is occupied by free nitrate anions and uncoordinated water molecules. Coordinated water molecules form strong H-bonds with free nitrate anions, and free water molecules lead to the H-bonds-based 3D structure. Interestingly, close examination of both structures showed that the M–M–M angles of both compounds are quite different, as the angle expanded from 101.09° (**1a**) to 106.61° (**1**) during structural transformation. This transformation leads to the drastic change in the shape and size of 1D channel (Figure 2). In single-crystal form, compound **1** is stable at room temperature for several hours, but in powder form, the compound is not stable and changes its structure in open air with time, which is evident from little variations of powder X-ray diffraction (PXRD) patterns of **1** at different time intervals. Thermo-gravimetric analysis (TGA) of the powder sample showed an approximately 5% weight loss at around 120°C, corresponding to approximately two water molecules per formula unit. Furthermore, TGA showed that the sample is stable up to around 300°C. To investigate the dynamic behavior of the framework, we studied the inclusion of different guest molecules into compound **1**. In a typical experiment, **1** was exposed to different dry solvents for a few days. PXRD analysis showed structural changes in the compound that were exposed to different vapors, suggesting the flexible behavior of the framework. For small hydrophobic guests (acetone, acetonitrile), PXRD patterns are identical, but different from the PXRD pattern of **1**, indicating new phases after guest inclusion. On the other hand, in the presence of small hydrophilic guests (ethanol, methanol), patterns were similar to that of **1**, indicating structural similarity. These results suggest different responses of **1** toward different types of guest molecules (Figure S12). To confirm the guest-inclusion behavior, solvent sorption experiments were carried out with hydrophobic and hydrophilic

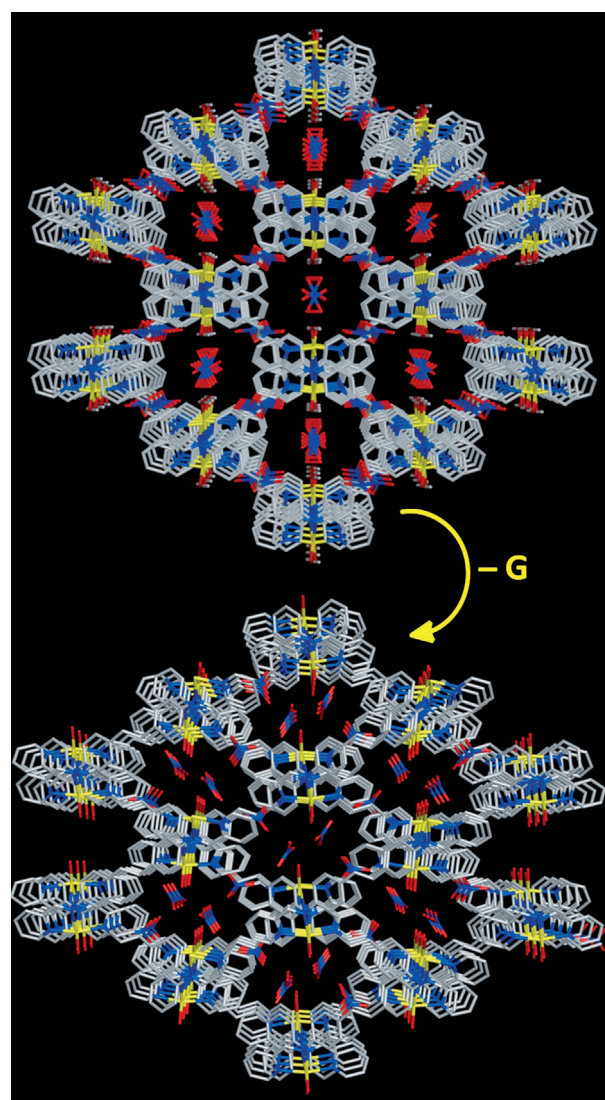


Figure 2. Perspective views of the structural transformation between compound **1a** and **1** (hydrogen atoms and free solvent molecules are omitted for clarity).

guests at 298 K (Figure 3). The dehydrated or guest-free phase (**1'**) was generated by heating **1** to 120°C for three hours to remove guest water molecules. The dynamic behavior of the framework was confirmed by these solvent sorption experiments. Small guest molecules of both types showed very similar sorption patterns. Little sorption was observed below $P/P_0=0.2$, but slowly increased with increasing pressure; all profiles show hysteric sorption behavior. Among hydrophilic guest molecules, water showed the highest amount of uptake ($\approx 143 \text{ mL g}^{-1}$), whereas methanol ($\approx 93 \text{ mL g}^{-1}$) and ethanol ($\approx 48 \text{ mL g}^{-1}$) showed less amount of uptake, in accordance with the size of the guest molecules (Figure S16). Small and similar-sized hydrophobic guests (acetonitrile and acetone) showed a similar amount of uptake ($\approx 160 \text{ mL g}^{-1}$), but large hydrophobic guest molecules (benzene and cyclohexane) could not enter into the channels because of the insufficient space inside the channels (Figure 3, and Figure S15 in the Supporting Information).

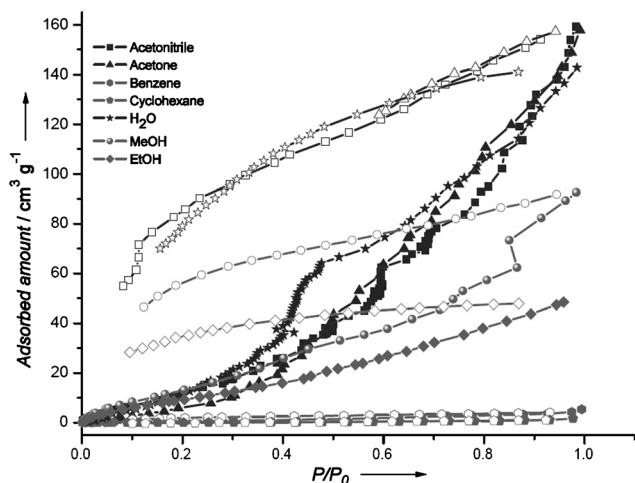


Figure 3. Sorption curves of hydrophobic (acetonitrile, acetone, benzene, cyclohexane) and hydrophilic (H_2O , MeOH, EtOH) guest molecules at 298 K. Filled shapes = adsorption, unfilled shapes = desorption.

The flexible nature of these framework was also observed in anion-exchange studies. As described above, the 1D channel along the c axis of compound **1** is filled with NO_3^- anions. To study the anion-dependent structural dynamism of the compound, we performed anion-exchange experiments. For this purpose, we used two types of anions: 1) anions with a weak or noncoordinating nature, such as ClO_4^- and $\text{N}(\text{CN})_2^-$ (type A), and 2) anions with a strong coordinating nature, such as N_3^- and SCN^- (type B). Crystals of compound **1** were immersed in separate methanolic solutions with an excess of NaN_3 , KSCN , NaClO_4 , and $\text{NaN}(\text{CN})_2$. We then monitored anion-exchange experiments by FT-IR spectroscopy. We observed that complete exchange of anions occurred within five days. FT-IR spectra of anion-exchanged products showed strong bands associated with exchanged anions, and the disappearance of bands of nitrate anions. Other bands in the spectra remained almost unchanged, suggesting that the frameworks of the complexes remained intact throughout the exchange process. Compound **1** with NO_3^- anions inside the channels (designated as $\mathbf{1} \supset \text{NO}_3^-$) shows a strong band at 1390 cm^{-1} , corresponding to nitrate anions, and this band almost completely disappeared in anion-exchanged products. New bands appeared at $\approx 2050 \text{ cm}^{-1}$ ($\mathbf{1} \supset \text{N}_3^-$), $\approx 2080 \text{ cm}^{-1}$ ($\mathbf{1} \supset \text{SCN}^-$), $\approx 1100 \text{ cm}^{-1}$ ($\mathbf{1} \supset \text{ClO}_4^-$), and $\approx 2160 \text{ cm}^{-1}$ ($\mathbf{1} \supset \text{N}(\text{CN})_2^-$) as expected for different anions (Figure 4). PXRD patterns of anion-exchanged products are different for different anions because of their different shape, size, and coordinating tendency, thus showing the highly flexible nature of the framework. The framework can easily adjust its channel dimension to encapsulate different guest anions because of its dynamic nature.

Reversibility of the anion exchange was studied in a two-stage experiment with two solutions of tetrabutylammonium nitrate in methanol (concentrations: 0.5 mM and 1.0 mM; see experimental details in the Supporting Information). In the first stage of the experiment, with a concentration of 0.5 mM NO_3^- in MeOH, FT-IR spectra showed that ClO_4^- was completely exchanged by NO_3^- , while $\text{N}(\text{CN})_2^-$, N_3^- , and

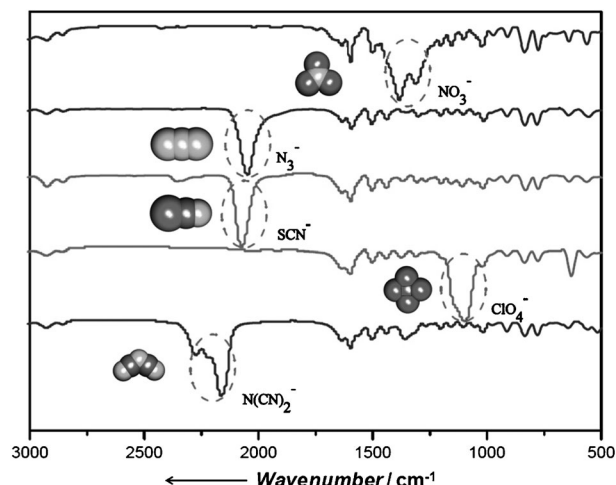


Figure 4. IR spectra of anion-exchanged compounds with highlighted band positions of the corresponding anions.

SCN^- were not exchanged (Figures S20 and 21). In the second stage of the experiment, with a concentration of 1.0 mM NO_3^- in MeOH, only little exchange of $\text{N}(\text{CN})_2^-$ by NO_3^- was observed, which was confirmed by the presence of an NO_3^- band in the FT-IR spectrum of $\mathbf{1} \supset \text{N}(\text{CN})_2^-$ and a slightly reduced band intensity of $\text{N}(\text{CN})_2^-$. On the other hand, no NO_3^- uptake into $\mathbf{1} \supset \text{N}_3^-$ and $\mathbf{1} \supset \text{SCN}^-$ was observed, suggesting strong interactions of N_3^- and SCN^- anions with the framework. However, $\mathbf{1} \supset \text{ClO}_4^-$ was again completely exchanged by NO_3^- , as in the previous experiment.

Selective anion exchange with the framework was investigated by performing anion-exchange experiments with different binary mixtures of anions. Five different binary combinations were used to study affinity, $\text{N}_3^-/\text{SCN}^-$, $\text{N}_3^-/\text{ClO}_4^-$, $\text{N}_3^-/\text{N}(\text{CN})_2^-$, $\text{ClO}_4^-/\text{N}(\text{CN})_2^-$, and $\text{SCN}^-/\text{N}(\text{CN})_2^-$. In a typical experiment, crystals of **1** were immersed in a methanolic solution of mixed anions in equimolar concentration (see experimental details in the Supporting Information). Anion exchange was further monitored by FT-IR analysis to examine preferential exchange from the mixture. Among the five combinations, $\text{N}_3^-/\text{SCN}^-$ and $\text{N}_3^-/\text{ClO}_4^-$ showed selective anion exchange with the framework. With $\text{N}_3^-/\text{SCN}^-$, NO_3^- is preferentially exchanged by SCN^- (Figure S22), and with $\text{N}_3^-/\text{ClO}_4^-$, NO_3^- is preferentially exchanged by N_3^- (Figure 5b). With the other combinations, the presence of both anions inside the framework was confirmed by their respective IR bands (Figures S24–26). It is worth noting that anion exchange could not be reverted in $\mathbf{1} \supset \text{SCN}^-$ and $\mathbf{1} \supset \text{N}_3^-$ because of strong coordination of the corresponding anions. Thus, the above-mentioned experiments show the order of affinity of guest anions to the framework: $\text{SCN}^- > \text{N}_3^- > \text{N}(\text{CN})_2^- > \text{ClO}_4^-$ (Figure 5a). These differences in affinity to the framework arise from several properties of the anions, such as their size, shape, geometry, their coordinating tendency to Zn^{II} , and also their different π - π interaction and hydrogen-bonding abilities with the framework.

Anion-exchanged materials showed interesting anion-dependent luminescent behavior (Figure 6a). Solid-state UV absorptions were measured for all anion-exchanged

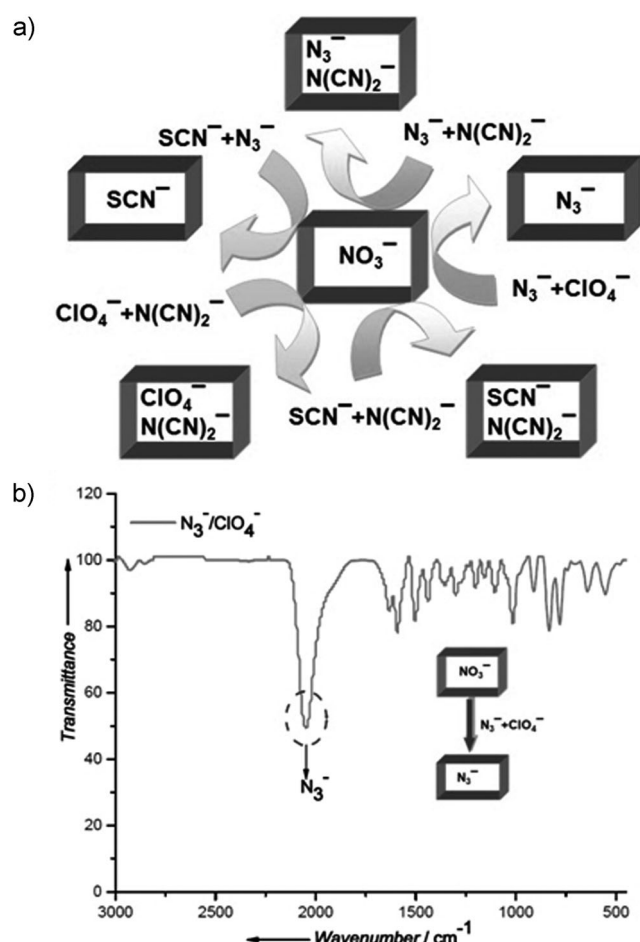


Figure 5. a) Schematic representation of the anion selectivity with combinations of two anions. b) Selective uptake of N_3^- from the combination of anions evidenced by FT-IR spectrum.

compounds, and these absorption curves were very similar to that of compound **1** (Figure S27). Furthermore, solid-state emission spectra of powder samples of **L**, **1**, and all anion-exchanged compounds were measured at room temperature (Figure 6b). Upon excitation at 394 nm, **L** shows two emission bands, at 512 nm and 533 nm; **L** is weakly fluorescent compared to the other samples. Compound **1** showed an intense band at 541 nm with a red-shift with respect to **L**, which may be attributed to the coordinating effect of **L** to Zn^{II} . Anion-exchanged compounds **1**⊃ N_3^- , **1**⊃ SCN^- , **1**⊃ $\text{N}(\text{CN})_2^-$, and **1**⊃ ClO_4^- display broad bands with intensity maxima at 514, 542, 543, and 536 nm, respectively. Compound **1**⊃ N_3^- showed a blue-shift with respect to **L** and **1**. In case of compound **1**, $\pi^*\text{-n}$ or $\pi^*\text{-}\pi$ intraligand transitions are possible. The emission intensity of anion-exchanged compounds was very different to the emission intensity of **1**. For anion-exchanged compounds of type A, that is, **1**⊃ $\text{N}(\text{CN})_2^-$ and **1**⊃ ClO_4^- , high enhancement of fluorescence was observed (70.72 and 84.14 % respectively), on the other hand, for anion-exchanged compounds of type B, that is, **1**⊃ N_3^- and **1**⊃ SCN^- , fluorescence quenching was observed (29.53 % and 80.36 %, respectively; Figure 6c).

Quantum yields were measured for **1** and anion-exchanged compounds in the solid state at room temperature

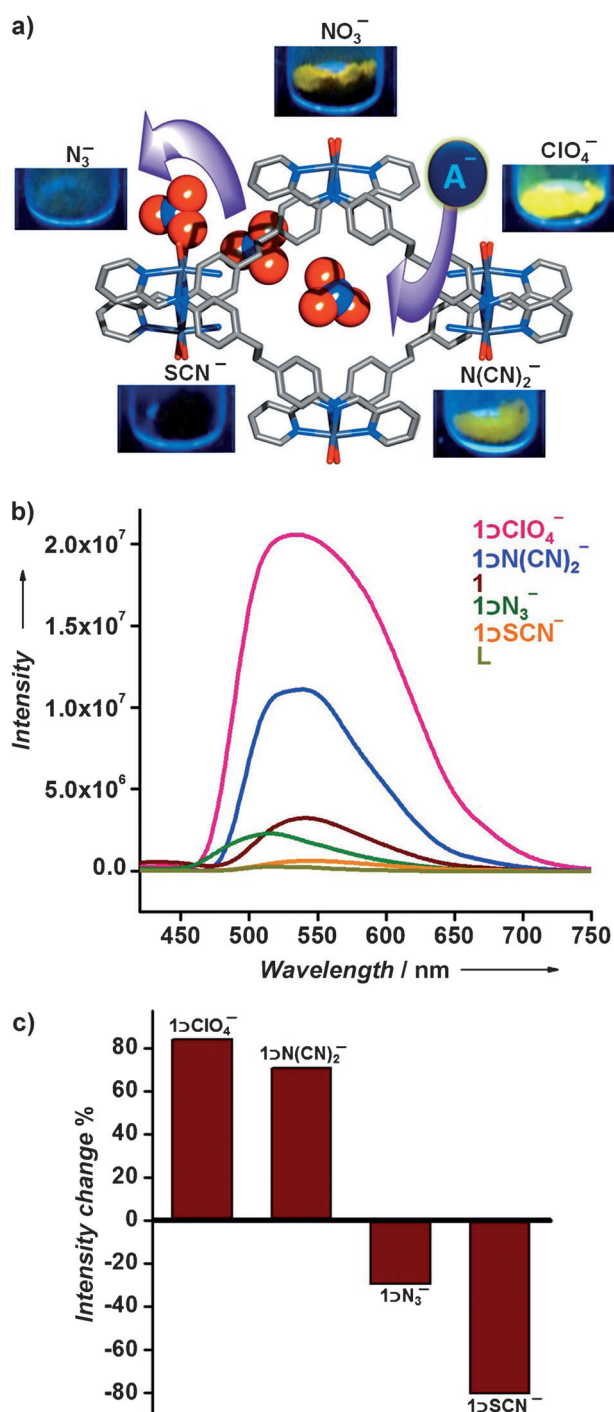


Figure 6. a) Effects of anion exchange on the solid-state luminescence properties of **1**. b) Luminescence intensity of different anion-exchanged samples. c) Bar diagram showing luminescence enhancement and quenching of anion-exchanged samples with respect to **1**.

using the technique for the powder samples described by Brill et al.,^[9] with the following expression:

$$\Phi_x = \frac{1 - R_{st}}{1 - R_x} \frac{I_x}{I_{st}} \Phi_{st} \quad (1)$$

R_x and R_{st} represent diffuse reflectance of the complex and the standard, respectively (with regard to a particular

wavelength). Φ_x and Φ_{st} are the quantum yields of solid samples and standard phosphor sample, respectively. I_x and I_{st} represent the integrated emission spectrum of the sample x and the standard, respectively. KBr was used as a reflecting standard, and perylene was used as a standard phosphor sample with an emission maximum at approximately 569 nm ($\Phi_{st} = 0.98$,^[10] excitation range 390 to 440 nm). The measured values of quantum yields of **1** and anion-exchanged compounds are in good agreement with their respective luminescence intensity profiles. **1**ClO₄[−] has the most intense emission profile ($\Phi = 0.921$), and **1**SCN[−] has the least intense emission profile ($\Phi = 0.0015$). Quantum yields of **1**N(CN)₂[−] and **1**N₃[−] are 0.357 and 0.0250, respectively, and in good agreement with their corresponding luminescence intensities. The reasons for the order of observed luminescence of the different anion-exchanged compounds are not very obvious; the differences are probably a result of various electronic interactions of the anions with the framework walls and the Zn^{II} center, depending upon their size, shape, geometry, and coordinating tendencies. As ClO₄[−] and N(CN)₂[−] are weakly coordinating, they can occupy different positions within the dynamic framework after exchange with NO₃[−], thus helping to change the framework in such a way that intraligand interactions may increase, and luminescence may subsequently be enhanced. As N₃[−] and SCN[−] are strongly coordinating with Zn^{II}, their coordination can lead to drastic structural change (also observed in PXRD, Figure S13), thus diminishing intraligand interactions within the framework, which may reduce luminescence intensity compared to compound **1**.

In conclusion, we have synthesized a dynamic luminescent cationic porous framework using a newly designed chelating N-donor ligand. The compound shows guest- as well as anion-dependent structural dynamic behavior. Guest-dependent dynamic behavior has been demonstrated by SCSC experiments. Anions of the compound encapsulated in the channels are completely exchangeable by other anions. Completely reversible, partially reversible, and nonreversible anion exchange was observed depending upon the nature of the anions. Furthermore, different kinds of affinities of the anions toward the framework were observed. Anion-exchanged compounds showed interesting anion-responsive tunable luminescent properties, which might have important biological and environmental applications.

Experimental Section

Synthesis of ligand L: The condensation of 4,4'-ethylenedianiline (5 g, 0.0235 mol) and 2-pyridine carboxaldehyde (5.034 g, 0.047 mol) in EtOH/MeOH (1:1, 100 mL) for 3 h at 70 °C led to a light-yellow solid, which was filtered, washed with EtOH and MeOH, and dried under vacuum to afford the product as a light-yellow solid (7 g). Calcd for C₂₆H₂₂N₄: C, 79.89; H, 5.67; N, 14.33; found: C, 80.40; H, 5.07; N, 14.52.

Synthesis of compound 1a: In a glass tube, benzene (1 mL) and a solution of Zn(NO₃)₂ (29.74 mg) in MeOH (1 mL) were carefully layered over a solution of **L** (39 mg) in CH₂Cl₂ (1 mL). Rod-like yellow crystals suitable for X-ray studies were obtained in approximately 60% yield after 15 days.

When parent crystals were taken out of the mother liquor and kept in open air for about 1.5 h, they changed to compound **1**. FT-IR

(KBr pellet): $\tilde{\nu}$ = 3406.42(m), 2921.91(w), 1630.18(w), 1599.65(m), 1502.91(w), 1384.21(s), 1156.59(w), 1101.12(w), 1019.91(m), 907.19(m), 847.26(m), 775.34(m), 639.08(m), 564.10 cm^{−1} (m).

Crystal data for **1a**: Formula C₂₈H₃₀N₆O₈Zn, monoclinic, space group C2/c, $a = 17.746(5)$, $b = 12.105(4)$, $c = 15.306(5)$ Å, $\beta = 90.244(7)^\circ$, $V = 3287.7(19)$ Å³, $Z = 4$, $T = 150(2)$ K, $R = 0.0608$, $wR_2 = 0.1933$, GOF = 1.087. Crystal data for **1**: Formula C₂₆H₃₀N₆O₁₀Zn, monoclinic, space group P2₁/n, $a = 15.305(4)$, $b = 10.6119(3)$, $c = 18.043(5)$ Å, $\beta = 93.120(7)^\circ$, $V = 2926.0(14)$ Å³, $Z = 4$, $T = 150(2)$ K, $R = 0.0480$, $wR_2 = 0.1182$, GOF = 1.041. CCDC 883148 (**1a**) and 883147 (**1**) contain the supplementary crystallographic data for this paper. These data can be obtained free of charge from The Cambridge Crystallographic Data Centre via www.ccdc.cam.ac.uk/data_request/cif.

Received: August 20, 2012

Published online: December 5, 2012

Keywords: anion exchange · cationic framework · dynamic framework · luminescence · sorption

- [1] a) H.-C. Zhou, J. R. Long, O. M. Yaghi, *Chem. Rev.* **2012**, *112*, 673–674; b) Q.-K. Liu, J.-P. Ma, Y.-B. Dong, *J. Am. Chem. Soc.* **2010**, *132*, 7005–7017; c) A. C. McKinlay, R. E. Morris, P. Horcajada, G. Ferey, R. Gref, P. Couvreur, C. Serre, *Angew. Chem.* **2010**, *122*, 6400–6406; *Angew. Chem. Int. Ed.* **2010**, *49*, 6260–6266; d) J. An, S. J. Geib, N. L. Rosi, *J. Am. Chem. Soc.* **2009**, *131*, 8376–8377; e) J. Y. Lee, O. K. Farha, J. Roberts, K. A. Scheidt, S. T. Nguyen, J. T. Hupp, *Chem. Soc. Rev.* **2009**, *38*, 1450–1459; f) L. Ma, J. M. Falkowski, C. Abney, W. Lin, *Nat. Chem.* **2010**, *2*, 838–846; g) Z. Guo, R. Cao, X. Wang, H. Li, W. Yuan, G. Wang, H. Wu, J. Li, *J. Am. Chem. Soc.* **2009**, *131*, 6894–6895; h) G. Li, W. Yu, Y. Cui, *J. Am. Chem. Soc.* **2008**, *130*, 4582–4583.
- [2] a) A. R. Millward, O. M. Yaghi, *J. Am. Chem. Soc.* **2005**, *127*, 17998–17999; b) S. M. Humphrey, J.-S. Chang, S. H. Jung, J. W. Yoon, P. T. Wood, *Angew. Chem.* **2007**, *119*, 276–279; *Angew. Chem. Int. Ed.* **2007**, *46*, 272–275.
- [3] S. Horike, S. Shimomura, S. Kitagawa, *Nat. Chem.* **2009**, *1*, 695–704.
- [4] a) N. Yanai, K. Kitayama, Y. Hijikata, H. Sato, R. Matsuda, Y. Kubota, M. Takata, M. Mizuno, T. Uemura, S. Kitagawa, *Nat. Mater.* **2011**, *10*, 787–793; b) C.-L. Chen, A. M. Beatty, *J. Am. Chem. Soc.* **2008**, *130*, 17222–17223; c) J.-P. Zhang, X.-M. Chen, *J. Am. Chem. Soc.* **2008**, *130*, 6010–6017; d) N. Yanai, T. Uemura, M. Inoue, R. Matsuda, T. Fukushima, M. Tsujimoto, S. Isoda, S. Kitagawa, *J. Am. Chem. Soc.* **2012**, *134*, 4501–4504.
- [5] a) K. S. Min, M. P. Suh, *J. Am. Chem. Soc.* **2000**, *122*, 6834–6840; b) B.-C. Tzeng, T.-H. Chiu, B.-S. Chen, G.-H. Lee, *Chem. Eur. J.* **2008**, *14*, 5237–5245; c) Q.-Y. Yang, K. Li, J. Luo, M. Pana, C.-Y. Su, *Chem. Commun.* **2011**, *47*, 4234–4236.
- [6] a) T. K. Maji, R. Matsuda, S. Kitagawa, *Nat. Mater.* **2007**, *6*, 142–148; b) J.-P. Ma, Y. Yu, Y.-B. Dong, *Chem. Commun.* **2012**, *48*, 2946–2948.
- [7] a) Y. Cui, H. Xu, Y. Yue, Z. Guo, J. Yu, Z. Chen, J. Gao, Y. Yang, G. Qian, B. Chen, *J. Am. Chem. Soc.* **2012**, *134*, 3979–3982; b) C. Wang, W. Lin, *J. Am. Chem. Soc.* **2011**, *133*, 4232–4235; c) J. An, C. M. Shade, D. A. Chengelis-Czegan, S. Petoud, N. L. Rosi, *J. Am. Chem. Soc.* **2011**, *133*, 1220–1223.
- [8] Y. Takashima, V. M. Martínez, S. Furukawa, M. Kondo, S. Shimomura, H. Uehara, M. Nakahama, K. Sugimoto, S. Kitagawa, *Nat. Commun.* **2011**, *2*, 168.
- [9] A. Bril, A. W. De Jager-Veenis, *J. Res. Natl. Bur. Stand. Sect. A* **1976**, *80A*, 401–407.
- [10] W. H. Melhuish, *J. Opt. Soc. Am.* **1964**, *54*, 183–186.